PROCEEDINGS OF SCIENCE

Measurement of the inclusive $t\bar{t}$ cross-section in pp collisions at $\sqrt{s}$ = 8 TeV with the ATLAS detector

PoS(EPS-HEP2017)750

Arwa Bannoura[*†]
Bergische Universitaet Wuppertal (DE)
E-mail: arwa.bannoura@cern.ch

The inclusive $t\bar{t}$ production cross-section is measured in the lepton+jets channel using 20.2 fb^{-1} of proton–proton collision data at a centre-of-mass energy of 8 TeV recorded with the ATLAS detector at the LHC. Major systematic uncertainties due to the modelling of the jet energy scale and b-tagging efficiency are constrained by separating selected events into three disjoint regions. In order to reduce systematic uncertainties in the most important background, the W+jets process is modelled using Z+jets events in a data-based approach. The inclusive $t\bar{t}$ cross-section is measured with a precision of 5.7 % to be $\sigma_{t\bar{t}} = 248.3 \pm 0.7\,(\text{stat.}) \pm 13.4\,(\text{syst.}) \pm 4.7\,(\text{lumi.})$ pb, assuming a top-quark mass of 172.5 GeV. The result is in agreement with the Standard Model prediction.

The European Physical Society Conference on High Energy Physics
5-12 July
Venice, Italy

[*]Speaker.
[†]On behalf of the ATLAS Collaboration

1. Introduction

The top quark is an elementary particle in the Standard Model of particle physics. Being the most massive known elementary particle, makes it very important to study its properties. These studies provide both a precise probe of the Standard Model and a window for physics beyond the Standard Model. In proton-proton collisions, the dominant production process of top quarks is pair production ($t\bar{t}$ production) via the strong interaction. The measurement of the production cross-section reported here is performed in the semileptonic decay mode (lepton+jets), where one W boson decays leptonically and the other W boson decays hadronically, i.e. ($t\bar{t} \rightarrow \ell\nu b + q\bar{q}'\bar{b}$) [1]. The analysis is based on data collected with the ATLAS detector at the LHC corresponding to an integrated luminosity of 20.2 fb^{-1} at a pp centre-of-mass energy of $\sqrt{s} = 8$ TeV. This analysis supersedes the previous measurement from the ATLAS collaboration which achieved a total uncertainty of 9.4 % using the same dataset [2]. The measurement is in agreement with the Standard Model theoretical prediction, which is $\sigma(pp \rightarrow t\bar{t}) = 253^{+13}_{-15}$ pb. [3].

2. Event selection

The ATLAS experiment is described in details here [4]. $t\bar{t}$ events in the lepton+jets channel are identified to include electrons and muons, jets, some of which are b-tagged for likely containing b-hadrons, and sizable missing transverse energy. The identification and reconstruction of physics objects are not mentioned here. Details can be found in References [5, 6, 7, 8, 9].

Selected events are required to have one isolated charged lepton, i.e. an electron or muon, with transverse momentum $p_T > 25$ GeV. Electrons are required to be within pseudo-rapidity $|\eta| < 2.47$, excluding the calorimeter overlap-region $1.37 < |\eta| < 1.52$. Muons are selected within $|\eta| < 2.5$. Events must have at least four jets with $p_T > 25$ GeV and $|\eta| < 2.5$. At least one of the jets has to be b-tagged. To enhance the fraction of events with a leptonically decaying W boson, events are required to have $E_{\mathrm{T}}^{\mathrm{miss}} > 25$ GeV and the transverse mass $m_{\mathrm{T}}(W)$ of the lepton - $E_{\mathrm{T}}^{\mathrm{miss}}$ system is required to be

$$m_{\mathrm{T}}(W) = \sqrt{2p_{\mathrm{T}}(\ell) \cdot E_{\mathrm{T}}^{\mathrm{miss}} \left[1 - \cos\left(\Delta\phi\left(\vec{\ell}, \vec{E}_{\mathrm{T}}^{\mathrm{miss}}\right)\right)\right]} > 30\,\mathrm{GeV}, \tag{2.1}$$

with $p_{\mathrm{T}}(\ell)$ the transverse momentum of the charged lepton and $\Delta\phi$ the angle in the transverse plane between the charged lepton and the $\vec{E}_{\mathrm{T}}^{\mathrm{miss}}$.

3. Backgrounds estimation and modelling

The dominant background to $t\bar{t}$ production is W+jets production. This analysis uses a sample defined from collision data to model the discriminant distribution shapes for this background, while the normalisation is determined in the final fit. The multijet background is also modelled using collision data but normalised using control regions. All other backgrounds, i.e. single top, Z+jets and diboson production, are determined using simulated events and theoretical predictions.

PoS(EPS-HEP2017)750

3.1 W+jets background

The method to obtain a modelling of the W+jets background shape from data is based on the similarity of the production and decay of the Z boson to that of the W boson. An almost background-free Z+jets sample is selected from data by requiring events to contain two opposite charged leptons of the same flavour, i.e. e^+e^- or $\mu^+\mu^-$. The dilepton invariant mass $m(\ell\ell)$ has to match the Z-boson mass ($80 \leq m(\ell\ell) \leq 102$ GeV). These events are then "converted" into W+jets events. This is achieved by boosting the leptons of the Z-boson decay into the Z boson rest-frame, scaling their momenta to that of a lepton decay from a W boson by the ratio of the boson masses (m_W/m_Z) and boosting the leptons back into the laboratory system. After this conversion, one of the leptons is randomly chosen to be removed, and the $\vec{E}_{\mathrm{T}}^{\mathrm{miss}}$ is re-calculated. Finally, the event selection cuts discussed in Sect. 2 are applied, except for the b-tagging requirement. In the following, this sample is referred to as the $Z$to$W$ sample.

3.2 Multijet background

In order to construct a sample of multijet background events, different methods are adopted for the electron and muon channels. The "jet-lepton" method [10] is used in the electron channel to model the background due to fake electrons using a dijet sample, where a jet that passes the selection cuts of a signal electron is selected to resemble the electron. The "anti-muon" method [10] is used in the muon channel. A dedicated selection on data is performed to enrich a sample in events that contain fake muons, by changing some of the muon identification cuts. The normalisation of the multijet background is obtained from a fit to the observed $E_{\mathrm{T}}^{\mathrm{miss}}$ in the electron channel or $m_{\mathrm{T}}(W)$ distribution in the muon channel.

4. Systematic uncertainties

Several sources of systematic uncertainties affect the $t\bar{t}$ cross-section measurement. In addition to the luminosity determination, they are related to the modelling of the physics objects, the modelling of $t\bar{t}$ production and the understanding of the background processes. All of them affect the yields and kinematic distributions (shape of the distributions) in the three signal regions. The systematic uncertainties are evaluated using pseudo-experiments. Details about the sources and evaluation of systematic uncertainties are explained in [1].

5. Extraction of the $t\bar{t}$ cross-section

Selected events are separated into three disjoint signal regions. SR1 ($\geq$ 4 jets, 1 b-tag) has the highest background fraction and the highest selected signal events. SR2 (4 jets, 2 b-tags) provides an unambiguous association of the reconstructed objects to the top-quark decay products. SR3 ($\geq$ 4 jets, $\geq$ 2 b-tags excluding events from SR2) has the smallest background fraction.

For the determination of the $t\bar{t}$ cross-section, a discriminant variable in each signal region is defined. The number of $t\bar{t}$ events is extracted using a simultaneous fit of all three discriminant distributions to observed data. In order to reduce systematic uncertainties due to the jet energy scale and b-tagging efficiency, their effects on the signal and background distributions are parametrised with nuisance parameters, which are included in the fit. The ratio of single to double b-tagged events, i.e. the ratio of events in SR1 and the sum of events in SR2 and SR3 together is sensitive to the b-tagging efficiency. In SR1 and SR3, the output distribution of an artificial neural network (NN) [11] is used. Seven variables are chosen as input to the NN. These variables are based on invariant masses between jets and leptons, event shape observables and properties of the reconstructed top quarks. For the training of the NN, an equal number of simulated $t\bar{t}$ events and $ZtoW$ events is used. The discriminating power of the NN between $ZtoW$ and $t\bar{t}$ events can be seen in Fig. 1(a) for SR1 . Since in SR2 the background contribution is very small, a different distribution

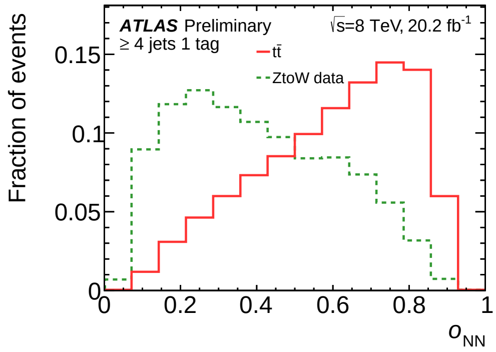

(a)

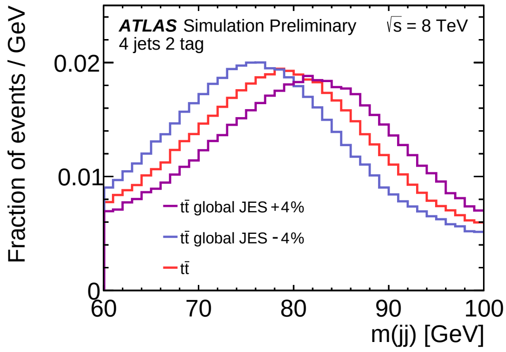

(b)

Figure 1: (a) Probability densities of the neural-network discriminant o_{NN} for the simulated $t\bar{t}$ signal process and the W+jets background process derived from data using converted Z+jets events for SR1 . (b) Probability densities for the $t\bar{t}$ signal process of the $m(jj)$ distribution for three different values of the JES, where events beyond the x-axis range are not shown and the range is restricted to show the peak [1].

is used as the discriminant in the final fit, which is the invariant mass of the two untagged jets $m(jj)$. The $m(jj)$ is frequently utilised in several measurements of the top quark mass to reduce the impact of the jet energy scale (JES) uncertainty [12]. The dependency of $m(jj)$ on the JES is shown in Fig. 1(b) using simulated $t\bar{t}$ events with modified JES correction factors. Here the energy of the jets are scaled by a constant scaling factor of 1.00 ± 0.04.

6. Result

The distributions of signal and background processes scaled and morphed to the fitted values are compared to the observed distributions of the NN discriminant distribution in SR1 and SR3 and the $m(jj)$ distribution in SR2, shown in Fig. 2. The total uncertainty in the inclusive $t\bar{t}$ cross-section is determined to be $\pm 5.7\,\%$. The largest uncertainty is due to the uncertainty in the PDF sets and the MC modelling of the signal process. The uncertainties in the JES and the b-tagging efficiency have been significantly reduced by including them as nuisance parameters together with the choice of the signal regions and the discriminant distributions.

The inclusive $t\bar{t}$ cross-sections is measured to be [1]:

$$\sigma_{t\bar{t}} = 248.3 \pm 0.7\,(\mathrm{stat.}) \pm 13.4\,(\mathrm{syst.}) \pm 4.7\,(\mathrm{lumi.})\ \mathrm{pb}$$

assuming a top-quark mass of $m_{\mathrm{top}} = 172.5\,\mathrm{GeV}$.

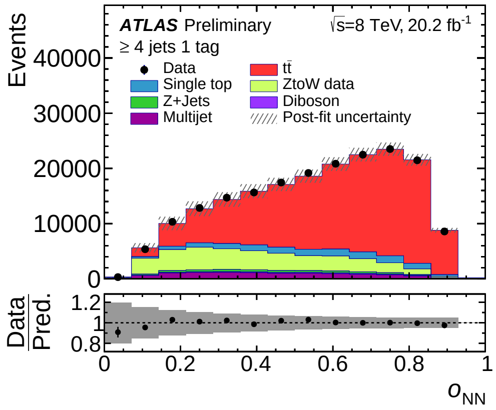

(a)

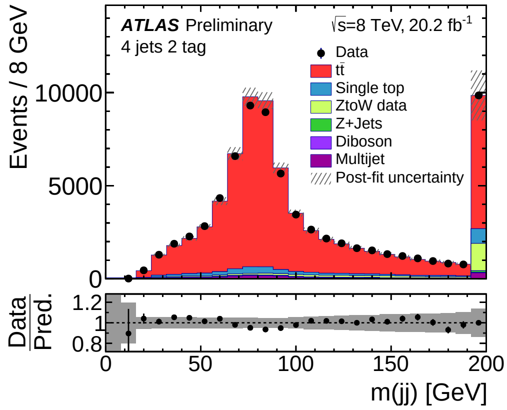

(b)

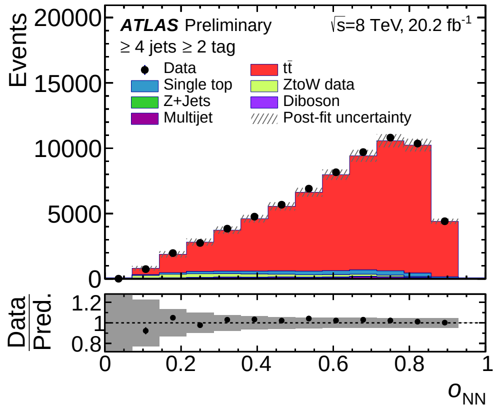

(c)

Figure 2: Neural network discriminant o_{NN} and the $m(jj)$ distributions normalised to the result of the maximum-likelihood fit for (a) SR1, (b) SR2, and (c) SR3. The hatched and gray error bands represent the post-fit uncertainty. The ratio of observed to predicted (Pred.) number of events in each bin is shown in the lower histogram. Events beyond the x-axis range are included in the last bin [1].

References

[1] ATLAS Collaboration, "Measurement of the inclusive $t\bar{t}$ cross-section in the lepton+jets channel in pp collisions at $\sqrt{s} = 8$ TeV at the ATLAS detector." ATLAS-CONF-2017-054, 2017.

[2] ATLAS Collaboration, *Measurement of the top pair production cross section in* 8 *TeV proton–proton collisions using kinematic information in the lepton+jets final state with ATLAS*, *Phys. Rev. D* **91** (2015) 112013, [1504.04251].

[3] M. Cacciari, M. Czakon, M. Mangano, A. Mitov and P. Nason, *Top-pair production at hadron colliders with next-to-next-to-leading logarithmic soft-gluon resummation*, *Phys. Lett. B* **710** (2012) 612–622, [1111.5869].

[4] ATLAS Collaboration, *The ATLAS Experiment at the CERN Large Hadron Collider*, *JINST* **3** (2008) S08003.

[5] ATLAS Collaboration, *Electron efficiency measurements with the ATLAS detector using 2012 LHC proton–proton collision data*, Eur. Phys. J. C **77** (2017) 195, [1612.01456].

[6] ATLAS Collaboration, *Measurement of the muon reconstruction performance of the ATLAS detector using 2011 and 2012 LHC proton–proton collision data*, Eur. Phys. J. C **74** (2014) 3130, [1407.3935].

[7] ATLAS Collaboration, *Jet energy measurement and its systematic uncertainty in proton–proton collisions at $\sqrt{s} = 7$ TeV with the ATLAS detector*, Eur. Phys. J. C **75** (2015) 17, [1406.0076].

[8] ATLAS Collaboration, *Performance of b-Jet identification in the ATLAS Experiment*, JINST **11** (2016) P04008, [1512.01094].

[9] ATLAS Collaboration, *Performance of algorithms that reconstruct missing transverse momentum in $\sqrt{s} = 8$ TeV proton–proton collisions in the ATLAS detector*, Eur. Phys. J. C **77** (2017) 241, [1609.09324].

[10] ATLAS Collaboration, "Estimation of non-prompt and fake lepton backgrounds in final states with top quarks produced in proton–proton collisions at $\sqrt{s} = 8$ TeV with the ATLAS Detector." ATLAS-CONF-2014-058, 2014.

[11] M. Feindt and U. Kerzel, *The NeuroBayes neural network package*, Nucl. Instrum. Meth. A **559** (2006) 190–194.

[12] ATLAS Collaboration, *Measurement of the top quark mass in the $t\bar{t} \to$ lepton+jets and $t\bar{t} \to$ dilepton channels using $\sqrt{s} = 7$ TeV ATLAS data*, Eur. Phys. J. C **75** (2015) 330, [1503.05427].